UNIVERSITY *of* York

This is a repository copy of *Antibody mimetics for the detection of small organic compounds using a quartz crystal microbalance*.

White Rose Research Online URL for this paper:
http://eprints.whiterose.ac.uk/111982/

Version: Accepted Version

White Rose
university consortium
Universities of Leeds, Sheffield & York

eprints@whiterose.ac.uk
https://eprints.whiterose.ac.uk/

Antibody mimetics for the detection of small organic compounds using a quartz crystal microbalance

SCHOLARONE™
Manuscripts

Antibody mimetics for the detection of small organic compounds using a quartz crystal microbalance.

ELENI KOUTSOUMPELI[§*], CHRISTIAN TIEDE[†], JAMES MURRAY[‡♦], ANNA TANG[†], ROBIN S. BON[‡#], DARREN C. TOMLINSON[†], STEVEN JOHNSON[§*]

[§]Department of Electronics, University of York, Heslington, York, YO10 5DD, United Kingdom

[†]School of Molecular and Cellular Biology, University of Leeds, Leeds, LS2 9JT, United Kingdom

[‡]School of Chemistry, University of Leeds, Leeds, LS2 9JT, United Kingdom

[#]School of Medicine, University of Leeds, Leeds, LS2 9JT, United Kingdom

*Tel: +44(0)1904 32 2693, Fax: +44 (0)1904 32 2335, E-mail: steven.johnson@york.ac.uk, eleni.koutsoumpeli@york.ac.uk

ABSTRACT: Conventional immunoassays rely on antibodies that provide high affinity, specificity and selectivity against a target analyte. However, the use of antibodies for the detection of small-sized, non-immunogenic targets, such as pharmaceuticals and environmental contaminants presents a number of challenges. Recent advances in protein engineering have led to the emergence of antibody mimetics that offer the high affinity and specificity associated with antibodies but with reduced batch-to-batch variability, high stability and *in vitro* selection to ensure rapid discovery of binders against a wide range of targets. In this work we explore the potential of Affimers, a recent example of antibody mimetics, as suitable bio-receptors for the detection of small organic target compounds, here methylene blue. Target immobilisation for Affimer characterisation was achieved using long-chained alkanethiol linkers coupled with oligoethyleneglycol (LCAT-OEG). Using quartz crystal microbalance with dissipation monitoring (QCM-D), we determine the affinity constant, K_D, of the methylene blue Affimer to be comparable to that of antibodies. Further, we demonstrate the high selectivity of Affimers for its target in complex matrices, here a limnetic sample. Finally, we demonstrate an Affimer-based competition assay, illustrating the potential of Affimers as bioreceptors in immunoassays for the detection of small-sized, non-immunogenic compounds.

Immunoassays are important bioanalytical tests used to identify and quantify the concentration of specific analytes and have found applications across clinical science, medical diagnostics, environmental monitoring, and fundamental research.[1] Conventional immunoassays rely on monoclonal or polyclonal antibodies to provide high affinity, specificity and selectivity against a relevant analyte. However, antibodies are large, complex proteins and only retain their functionality and stability within a narrow range of conditions.[2] Moreover, antibody production and development is an expensive and time-consuming process, requiring the use of animals or mammalian cell cultures. Although monoclonal antibodies have been able to address the issue of batch-to-batch variability of polyclonal antibodies, the time, efforts and costs of hybridoma development are high.[3] In addition, due to the *in vivo* nature of these processes, the development of antibodies against non-immunogenic targets can be challenging. For example, many environmental contaminants, such as pesticides, toxins or pharmaceuticals are often too small or toxic for raising antibodies *in vivo*, limiting the development of immunoassays for many current and emerging contaminants.[4]

Recent advances in protein engineering have led to the emergence of antibody mimetics that can be selected *in vitro* to provide high affinity binders, but with increased stability and reduced costs and time of development. Affimers (previously described as Adhirons) are a recent example of these synthetic binding molecules.[5] Affimers are based on a consensus sequence of phytocystatins, where the inhibitory sequences have been replaced with randomised peptide sequences enabling the construction of a large and highly variant library of binding proteins (10^10 clones). The Affimer scaffold is significantly more stable than traditional antibodies, exhibiting a melting temperature of over 100 °C. The selection of Affimers against a specific target is achieved *in vitro* using phage display with high stringency washing to ensure Affimers with high binding affinity and selectivity. For example, we have selected Affimers against the yeast Small Ubiquitin-like Modifier (SUMO) protein that displayed very high affinity, comparable to that of antibodies, and high specificity enabling differentiation between yeast SUMO and the closely related human SUMO proteins.[5]

The *in vitro* nature of selection also enables the production of Affimers against a wide range of conventional and unconventional targets. For example, we have demonstrated selection of Affimers against over 350 different target proteins as well as peptides, cells, organic molecules and even inorganic metallic nanoparticles,[6-9] highlighting the versatility of this approach. *In vitro* selection also allows the development of Affimers against targets

for which raising antibodies is hard or even impossible, including non-immunogenic or highly toxic targets. This is critical for the future development of immunoassays for monitoring emerging contaminants in the environment or for quantifying the concentration of pharmaceuticals in a patient sample.

We present the first demonstration of an Affimer-based immunoassay for the quantification of small organic molecules, focusing on methylene blue (MB). MB is a water-soluble dye belonging to the phenothiazine class of heterocyclic compounds and its cationic charge and aromatic moieties offer interaction domains with an Affimer binding site. MB is used widely as a therapeutic agent and a stain for biochemical research,[10] and is also the most commonly used substance for dying cotton, wood and silk.[11] Therefore, although not highly toxic, its widespread release in the aquatic environment renders it an important environmental contaminant.[11] Given the small molecular mass of environmental contaminants such as MB, immunosensors for environmental monitoring are typically operated as competition assays where the binding reaction is effectively amplified. This requires approaches to immobilize the small molecule target onto a surface.

Here, we demonstrate an approach for immobilizing the small molecule targets using a self-assembled monolayer (SAM) of long-chained alkanethiols (LCAT) containing a MB-labelled oligoethyleneglycol component (OEG). Details of the solid-phase synthesis of LCAT-OEG-MB have been reported previously.[12] The LCAT component ensures the assembly of a dense and well-ordered molecular monolayer, while the OEG region increases the resistance of the molecular film to non-specific adsorption of molecules contained in a complex matrix, such as surface water samples. The assembly and structure of the molecular monolayer was assessed using electrochemistry (cyclic voltammetry and impedance spectroscopy) and FT-IR. Finally, we used QCM-D to investigate the kinetics, affinity and selectivity of Affimers for binding to the surface immobilised MB target and demonstrate the possibility of operation in a competition format. While we focus here on MB, the approaches developed here are generic and applicable to a range of targets and biosensor technologies. Our manuscript thus demonstrates the potential of Affimers as suitable bio-receptors for the detection of small organic compounds in aquatic samples.

EXPERIMENTAL SECTION

MATERIALS. *N*-18-(*N*-(carboxypropyl)methylene blue)-3,6,9,11,15-pentaoxaheptadecyl-11-mercaptounadecamide (LCAT-OEG-MB, Figure 1d) and *N*-(carboxypropyl)methylene blue were synthesised as described by Murray et al.,[12] and stored in ethanol at 1 mM concentration (-18 °C). Chemicals were purchased from Sigma-Aldrich (Gillingham, UK), unless noted otherwise. 29-mercapto-3,6,9,12,15,18-hexaoxanonacosan-1-ol (LCAT-OEG-OH; Figure 1c) was purchased from Prochimia Surfaces (Gdansk, Poland). Methylene blue chloride was purchased from Acros Organics (Geel, Belgium). *O*-(2-Aminoethyl)-*O*′-[2-(biotinylamino)ethyl]octaethylene glycol (referred to as biotin-PEG$_{(8)}$-NH$_2$) and 1-dodecanethiol 98% (Figure 1b) were purchased from Sigma-Aldrich. All buffers and solutions were prepared using ultrapure water (18.2 MΩ·cm, Milli-Q systems, Millipore) and the pH was measured using a pH meter (Mettler-Toledo, Switzerland).
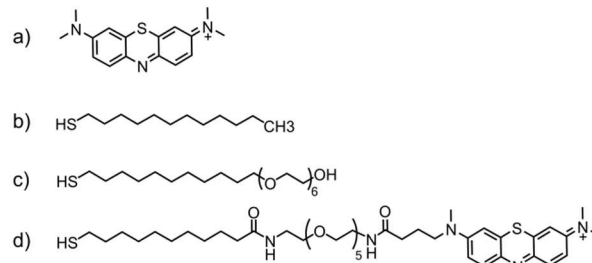

Figure 1. a) methylene blue, b) 1-dodecanethiol, c) LCAT-OEG-OH and d) LCAT-OEG-MB

AFFIMER DEVELOPMENT: PHAGE DISPLAY AND ELISA. *N*-(carboxypropyl) methylene blue was synthesised as in Murray et al.,[12] and biotinylated by NHS/EDC coupling with biotin-PEG$_{(8)}$-NH$_2$ (Supplementary Method 1). Phage display was performed as previously described but over five panning rounds.[5] In brief, for the first panning round, the biotinylated MB was bound to streptavidin-coated wells (Pierce, Loughborough, UK) for 1 hour, then 10^{12} cfu pre-panned phage were added for 2.5 hours with shaking. Panning wells were washed 10 times and eluted with 50 mM glycine, then 100 mM triethylamine for 6 min prior to infecting ER2738 cells for 1 hour at 37 °C with shaking followed by plating onto LB agar plates with 100 μg/mL carbenicillin and grown overnight. Colonies were scraped, inoculated in 25 ml of 2TY with carbenicillin and infected with ca. 1 x 10^9 M13K07 helper phage. After 16 hours the phage supernatant was incubated with biotinylated MB bound to streptavidin magnetic beads (Invitrogen, Paisley, UK) and eluted and amplified as above, for the second pan. The third panning round was performed on neutravidin high binding capacity wells (Pierce, Loughborough, UK) and eluted as above. The fourth and five panning rounds were performed on streptavidin and neutravidin coated plates as described above.

PHAGE ELISA. Individual ER2738 colonies were grown in 100 μL of 2TY with 100 μg/mL of carbenicillin in a 96-deep well plate at 37 °C (900 rpm) for 6 hours. A 25 μL aliquot of the culture was added to 200 μL of 2TY containing carbenicillin and grown at 37 °C (900 rpm) for 1 hour. Helper phage (10 μL of 10^{11}/mL) were added, followed by kanamycin to 25 μg/mL overnight and incubated at 25 °C (450 rpm). Streptavidin-coated plates were blocked with 2 × casein blocking buffer (Sigma-Aldrich, Gillingham, UK) overnight at 37 °C. The plates were incubated with biotinylated MB for 1 hour, and 45 μL of growth medium containing the phage was added and incubated for 1 hour. Following washing, phage were detected by a 1 : 1000 dilution of HRP-conjugated anti-phage antibody (Seramun, Heideesee, Germany) for 1 hour, visualised with 3,3′,5,5′-tetramethylbenzidine (TMB) (Seramun, Heidesee, Germany) and measured at 620 nm.

TARGET IMMOBILISATION. Planar gold surfaces, fabricated by electron beam evaporation of 25 nm Ti/100 nm

Au onto a cleaned Si wafer (IDB technologies, Wiltshire, UK), were functionalised with pure or mixed LCAT-OEG monolayers. Prior to functionalisation, the wafers were cleaved to 10 by 20 mm (20 by 30 mm for PM-IRRAS) and cleaned by immersion in Piranha solution (H_2SO_4:H_2O_2 70:30) for 10 min, followed by sonication in water and ethanol for 10 min each. (Note: Extreme caution must be taken when handling piranha solution, since it is strongly acidic and a strong oxidiser).

Pure LCAT-OEG-MB and LCAT-OEG-OH SAMs (also referred to as MB SAM and OH SAM respectively) were formed by immersion of the cleaned Au-coated substrates in a 0.1 mM ethanolic solution of the corresponding compound for 48 hours. Similarly, a mixture of LCAT-OEG-MB and LCAT-OEG-OH in a 1:3 ratio was used to prepare a mixed SAM (also referred to as MB:OH SAM). After incubation, the functionalised substrates were gently rinsed with ethanol and dried with N_2 gas.

ELECTROCHEMISTRY (CV, EIS). The SAM-functionalised Au working electrode was mounted in a three electrode electrochemical cell (Pt counter electrode and Ag/AgCl (saturated KCl) reference electrode). Contact to the working electrode was achieved using a spring loaded pin connector. A Viton O-ring defined the surface area exposed by the cell which was equal to 9.1 mm². Electrical impedance spectroscopy (EIS) and cyclic voltammetry (CV) were performed using a Bio Logic SP-300 potentiostat. Electrochemical measurements were performed in 100 mM sodium phosphate buffer pH 7 (PB 7).

POLARISATION MODULATION - REFLECTION ABSORPTION SPECTROSCOPY (PM-IRRAS). Infrared spectra of the LCAT-OEG SAMs were acquired using a Bruker Vertex70 spectrometer (Bruker UK Ltd, Coventry, UK) coupled with a PMA50 polarisation modulation unit (Hinds Instruments, Oregon, USA). The incident angle was set at 80° with a 4 cm⁻¹ spectral resolution, while the PEM controller operated at 1000 cm⁻¹. Average measurement time was 15 min, collecting 1000 scans. As reference, 1-dodecanethiol SAMs (referred to as C_{12} SAM) were prepared using the same immobilisation protocol as for LCAT-OEG SAMs.

QUARTZ CRYSTAL MICROBALANCE WITH DISSIPATION MONITORING (QCM-D). Gold coated QCM-D sensors (QSX 301, Biolin Scientific, Stockholm, Sweden) were cleaned by sonication in a 2% Hellmanex III solution (Hellma Analytics, Müllheim, Germany) and thorough rinsing in ultrapure water, followed by UV-ozone treatment (30 min) and immersion in EtOH (30 min). Cleaned sensors were functionalised with LCAT-OEG SAMs (mixed MB:OH 1:3 ratio or OH SAM) by 48 hours immersion to 0.1 mM ethanolic solutions. The LCAT-OEG-OH was selected for its well-established high protein resistance[13,14] and was used either as a control SAM to monitor potential non-specific interaction of Affimers with the surface, or as a SAM dilutant to separate the bulky redox MB tail groups.

Following fuctionalisation, the sensors were gently rinsed in EtOH, dried with N_2 gas and loaded into the QCM-D flow modules (QSense E4, QFM 401, Biolin Scientific, Stockholm, Sweden). The surface area exposed to solution was equal to 0.95 cm² as defined by a Viton O-ring. The temperature in the QCM-D chamber was controlled by a peltier device and was set to 16 °C (standard deviation 5×10⁻³ °C) for all measurements. Resonant frequency (F) and dissipation (D) were monitored while ultrapure water was passed over the sensors using a peristaltic pump at a flow rate of 20 µL/min, until a steady baseline was achieved (defined by a frequency shift of less than 1 Hz over 10 minutes), followed by PB 7 to establish a running buffer baseline. Next, MB-Affimer solutions in PB 7 were introduced at 20 µL/min flow rate until the frequency saturated. Affimers raised against green fluorescent protein (GFP) were used as controls (referred to as GFP-Aff). Finally, the sensors were washed with PB 7. For binding kinetics measurements, the flow rate was set at 10 µL/min.

Electrochemical QCM-D (EQCM-D) was performed using the QEM 401 electrochemistry module (Biolin Scientific, Stockholm, Sweden) which includes a stainless steel counter electrode, a low leak Ag/AgCl reference electrode and a contact to the working electrode, here a gold coated sensor (QSX-338, Biolin Scientific, Stockholm, Sweden). Electrochemical measurements were performed using a Bio Logic SP-200 potentiostat. The peristaltic pump was paused for 5 min before performing cyclic voltammetry.

To study the selectivity of MB-Affimers (that is the ability to recognise MB among the interferences in a sample), limnetic samples were collected (Heslington, York, UK), syringe-filtered through a 0.22 µM sterile filter unit (Millex, Millipore, Cork, Ireland) and used as a running buffer (measured pH 8.17±0.01).
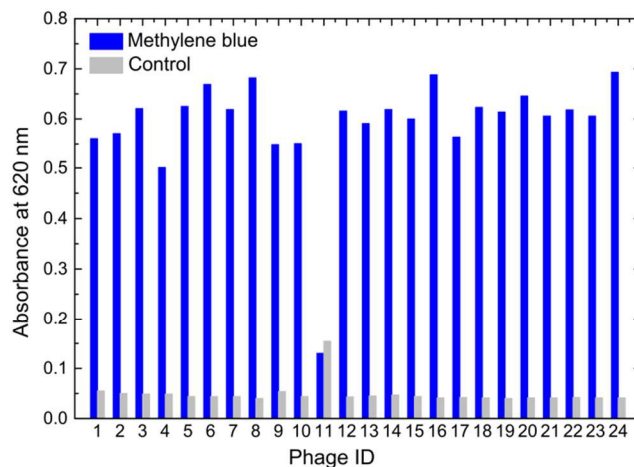

Figure 2. Phage ELISA of Affimers from 24 clones incubated in streptavidin-coated wells previously treated with biotinylated MB (blue), showing the TMB product absorbance (620 nm). Control (grey): streptavidin-coated wells (no MB).

Table 1. Sequences of Affimer binding sites

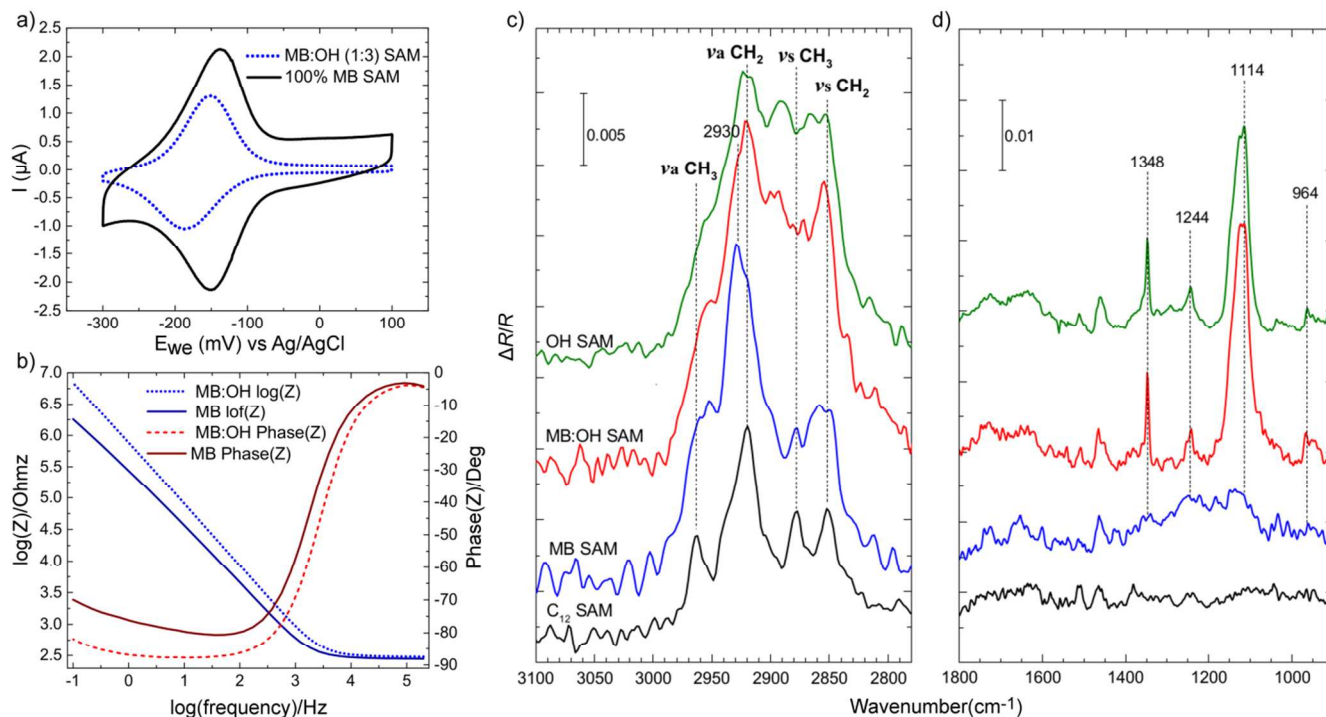|	Loop sequence 1	Loop sequence 2
MB-Aff1	WGWVYTMGD	FNSTPPWNV
MB-Aff2	YKHQWGYW	WAHDDAGFF
MB-Aff5	WGYQEKKVY	FDESMPWPM

Figure 3. a) Cyclic voltammograms of MB SAM and MB:OH SAM in PB7 at a scan rate of 250 mV/s, b) Electrochemical impedance spectroscopy of MB SAM and mixed MB:OH SAM (1:3) in PB 7, c-d) PM-IRRAS spectra of LCAT-OEG and alkanethiol SAMs on gold, showing c) the CH stretch region (2750-3100 cm⁻¹) and d) the fingerprint region (900-1800 cm⁻¹).

RESULTS AND DISCUSSION

AFFIMER DEVELOPMENT. Phage display was used to isolate Affimer reagents from a highly diverse Affimer library that bind to MB.[5] After five panning rounds, 24 individual colonies were isolated (each containing a monoclonal Affimer binder), and a phage ELISA was performed to identify those that bind to MB (Figure 2). Out of the 24 isolated reagents, 23 showed binding to the target by ELISA, of which 3 unique reagents were isolated; MB-Affimer-1 (MB-Aff1), MB-Affimer-2 (MB-Aff2) and MB-Affimer-5 (MB-Aff5). The binding loops sequences are shown in Table 1 (entire sequence including Affimer scaffold and binding loop are included in Supplementary Data 1). Of these, MB-Aff1 and MB-Aff5 were the most common and contained sequence homology in both loops. However, MB-Aff5 demonstrated the highest levels of expression and was thus taken forward for in depth analysis.

MB SAM CHARACTERISATION. Prior to investigating Affimer binding, it was necessary to confirm that the immobilisation of MB through SAMs on Au surfaces does not alter the properties of the target and that the conformation of the SAM is such that the target is presented efficiently for Affimer binding. We thus employed cyclic voltammetry to probe the redox properties of MB assembled in the MB SAM. The formation and structure of the monolayer was assessed using electrical impedance spectroscopy and FT-IR measurements using PM-IRRAS.

ELECTROCHEMISTRY (CV, EIS). Cyclic voltammograms of pure MB and mixed MB:OH SAMs are shown in Figure 3a. Characteristic of an ideal and reversible surface-immobilised redox system, the MB SAM exhibited symmetric redox peaks with minimal peak splitting

(I_{pa}/I_{pc}=1.2, ΔE_p= 7.7 mV). These findings are consistent with previous studies of MB SAMs[12,15] and confirm that MB retains its redox properties when incorporated in an LCAT-OEG monolayer. The oxidation and reduction peak current of the mixed SAM was lower than that of the pure MB SAM, due to dilution of redox groups in the mixed monolayer. From the linearity between the peak current and scan rate, we estimate the surface coverage of MB in the mixed MB:OH SAM to be 3.9×10^{12} molecules/cm². We note, the density of MB in the MB SAM was 1.4×10^{13} molecules/cm². While greater than the mixed SAM, this is lower than the density predicted for an ideal LCAT SAM.[16,17] EIS data for both the MB and mixed MB:OH SAM are shown in the Bode plot of Figure 3b. At 0.1 Hz, the phase angle for the mixed MB:OH SAM (-81.93°) suggests a dense, highly insulating monolayer that is almost free of pinholes and defects. In contrast, the minimum phase angle for the MB SAM is only -69.95°, typical of a monolayer of low packing density. The reduced packing density is likely due to the amorphous conformation of the OEG component as well as steric hindrance caused by the MB-tail groups.

PM-IRRAS: LCAT REGION. PM-IRRAS was used to better understand the observed differences in packing density. As shown in Figure 3c, the reference C_{12} SAM exhibited well-defined IR absorption peaks at the expected CH_3 and CH_2 symmetric (v_s) and asymmetric stretch (v_a) bands, characteristic of a tightly-packed, highly crystalline alkanethiol SAM with all-trans alkyl chains and very little gauche defects (v_a CH_2 2919 cm⁻¹ , v_s CH_2 2851 cm⁻¹, v_a CH_3 2963 cm⁻¹, v_s CH_3 2877 cm⁻¹).[18,19] The v_a CH_2 stretch in particular, is an indicator of the crystallinity of the molecular film,[18,20] and its presence in all LCAT-OEG SAMs
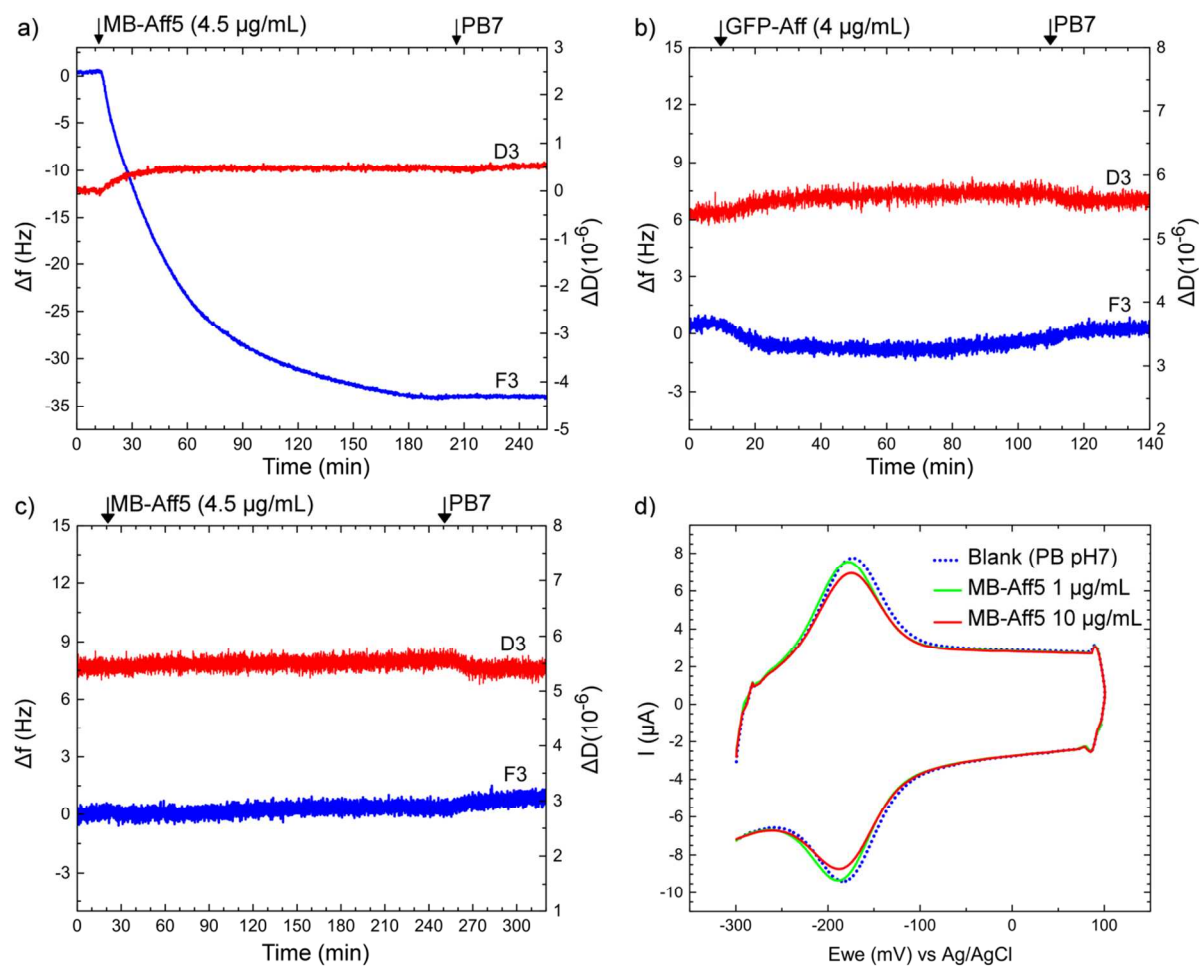
Figure 4. a-d) Real-time QCM-D showing changes in the resonant frequency (third harmonic, F3) and dissipation (D3) over time. QCM-D sensors functionalised with a) mixed MB:OH SAM treated with 4.5 µg/mL MB-Aff5, b) mixed MB:OH SAM treated with 4 µg/mL GFP-Aff, c) 100% OH SAM treated with 4.5 µg/mL MB-Aff5. d) Cyclic voltammograms (100 mV/s) of a MB:OH SAM-functionalised EQCM-D sensor at 0, 1 and 10 µg/mL MB-Aff5. PB 7 was used as running buffer in all measurements.

confirmed the existence of an all-trans LCAT component under the OEG layer.

PM-IRRAS: OEG REGION. IR absorption peaks characteristic of a helical OEG component (1348, 1244, 1114 and 964 cm^{-1})[18] are all clearly observed in the OH SAM and MB:OH SAM (Figure 3d). In particular, the intense and sharp absorption peak at 1114 cm^{-1} is typical of a highly crystalline OEG layer, with the OEG helices orientated almost parallel to the surface normal.[19,20] We note, while the OEG component in both OH SAM and MB:OH SAM is mostly highly ordered, the detection of several low intensity peaks and/or shoulders in the asymmetric C-O-C stretching region (for example at ~1124 or ~1080 cm^{-1}) suggests the existence of some amorphous-like OEG regions.

In contrast, the C-O-C stretch region of the pure MB SAM appeared as a broad, low intensity band corresponding to a highly amorphous OEG conformation.[19] Moreover, the 1348 cm^{-1} band, typical of the CH$_2$ wagging mode of a helical OEG was observed as a sharp, intense peak for both the OH and MB:OH SAMs, whereas for the MB SAM it appeared as a weak doublet at ~1360 and 1340 cm^{-1}, indicative of a more amorphous conformation. The reduced ordering of the OEG phase in the MB SAM can also be observed in the CH$_2$ stretch region (Figure 3c) where the presence of a 2930 cm^{-1} shoulder (v_a CH$_2$ stretch of an

amorphous OEG phase) in both MB and MB:OH SAMs, indicates a higher ratio of amorphous to helical OEG conformation in these SAMs compared to the OH SAM.[19] The dominance of an amorphous OEG phase in the MB SAM is attributed to steric hindrance caused by the bulky MB units that interfere with the ordered packing of the OEG layer. It is likely that the differences in the EIS spectra observed in Figure 3b are also related to the differences in helical to amorphous OEG ratio between the MB SAM and the mixed MB:OH SAM.

AFFIMER-METHYLENE BLUE INTERACTIONS. QCM-D coupled with electrochemistry (EQCM-D) was used to explore molecular interactions between MB-Aff5 and MB immobilised on the surface via the mixed MB:OH SAM. Real-time QCM-D data following exposure of a mixed MB:OH SAM (1:3) to a 4.5 µg/mL MB-Aff5 solution is shown in Figure 4a. The interaction of MB-Aff5 with MB leads to a significant decrease in the resonant frequency of the quartz sensor as a result of the increase in the mass deposited on the surface (the third harmonic (F3) is shown here). The average frequency shift due to MB-Aff5 binding is -29.54±2.11 Hz (from six nominally identical measurements). In vacuum, the resonant frequency of QCM-D is related to the mass loading of the crystal according to the Sauerbrey equation,[21] $\Delta m = -C \cdot \Delta f / n$. This

corresponds to an estimated deposited mass of 174.31 ±12.44 ng/cm² and translates to a surface coverage of 8.47(±0.6)×10¹² molecules/cm² for a 12.4 kDa Affimer (Supplementary Note 1). Although, the Sauerbrey model does not account for the viscoelasticity of the layer, here, the dissipation shift was sufficiently low ($\Delta D < 0.5 \cdot 10^{-6}$) to assume a dense, rigid film that couples to the oscillation of the quartz crystal. However, it should be noted, that, in the liquid phase, the resonant frequency is sensitive to a number of solution and interfacial factors, as described by Kanazawa and Gordon, 1985,[22] so the actual mass loading can differ from that estimated by Sauerbrey.

To rule out any non-specific interactions of Affimers with the monolayer or surface, a 100% OH SAM was challenged with the same MB-Aff5 solution and as shown in Figure 4c, the resonant frequency remained constant. We note, the absence of interaction between MB-Aff5 and the OH-SAM confirms the anti-fouling properties of the OEG region. The specificity of the interaction between MB and MB-Aff5 was further confirmed by exposure of a mixed MB:OH SAM to GFP-Aff (control Affimer) and, as seen in Figure 4b, the frequency and dissipation shifts were again insignificant and quickly recovered following rinsing in PB 7.
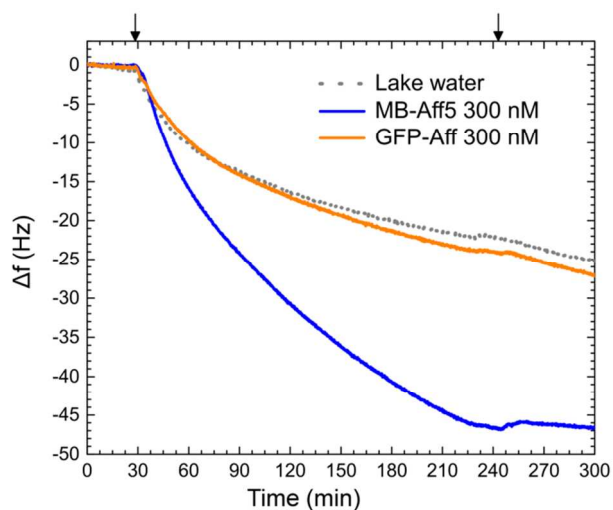

Figure 5. Real-time QCM-D of shifts in the resonant frequency (third harmonic) of MB:OH SAM-functionalised sensors during introduction of 300 nM MB-Aff5 in limnetic samples. Lake water was used as blank and 300 nM GFP-Aff in the same matrix was used as a control.

Interactions between MB-Aff5 and the surface-immobilised MB were also observed by monitoring the redox activity of MB in the monolayer. Figure 4d shows cyclic voltammograms of a MB:OH SAM-functionalised EQCM-D sensor before and after exposure to MB-Aff5. Here, binding of Affimers on the SAM limits the access of ions and/or protons from solution, resulting in a reduction in the peak oxidation and reduction current (I_{pa} and I_{pc}). The reduction in peak current was found to be dependent on MB-Aff5 concentration (Figure 4d) suggesting the potential for electrochemical detection and quantification of Affimer binding to redox-active targets.

AFFIMER-METHYLENE BLUE INTERACTIONS IN LIMNETIC SAMPLES. The MB-Aff5 and MB interactions observed by QCM-D and CV were measured in the controlled environment of a pure aqueous buffer solution. For environmental monitoring it is necessary that Affimers selectively bind their target in a more complex sample matrix, such as surface water samples.
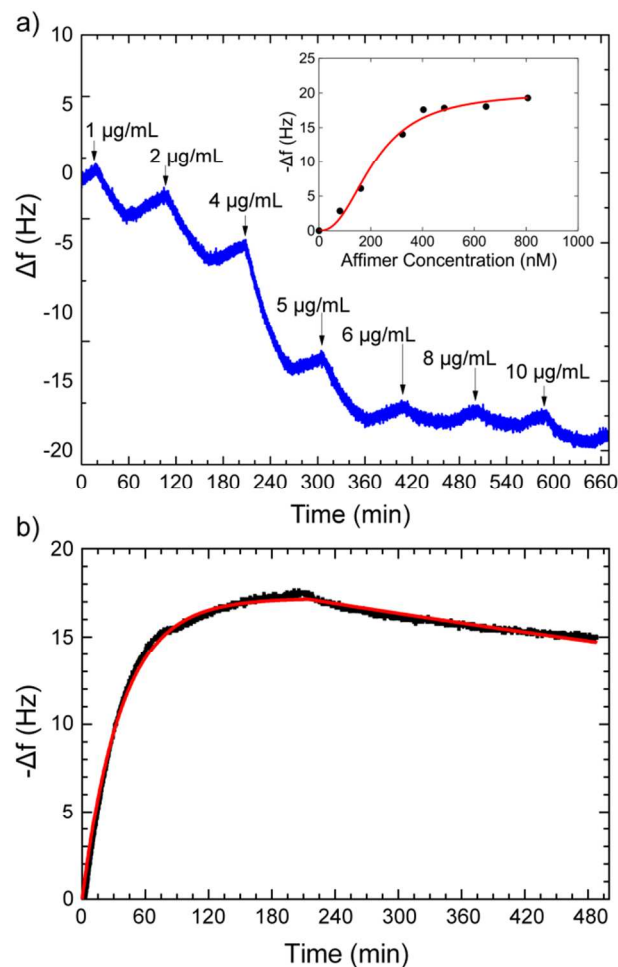

Figure 6. a) Saturation binding: real-time QCM-D of resonant frequency shifts Δf (third harmonic) of MB:OH SAM-functionalised sensors during introduction of increasing concentrations of MB-Aff5. Insert: frequency shift plotted against MB-Aff5 concentration (red line: Hill-Langmuir fitting); b) MB-Aff5 binding kinetics: real-time QCM-D of frequency shift of MB:OH SAM-functionalised sensors during injection of 8 μg/mL (645 nM) MB-Aff5 at 10 μL/min flow rate. Red line shows association-dissociation fitting curve.

The selectivity of MB-Aff5 was studied using limnetic samples as the running solvent. As shown in Figure 5, a significant increase in mass was observed following exposure of the MB:OH SAM-functionalised QCM-D sensor surface to the limnetic sample spiked with MB-Aff5. The shift in frequency is 1.5 times greater than that observed following exposure of the same SAM to a blank limnetic sample (i.e. free from Affimers). This difference suggests that despite the interferences in the sample, the MB-Aff5 binders were still able to effectively bind to MB. This was further supported using the GFP=Aff control binders spiked into limnetic sample, which led to a shift in
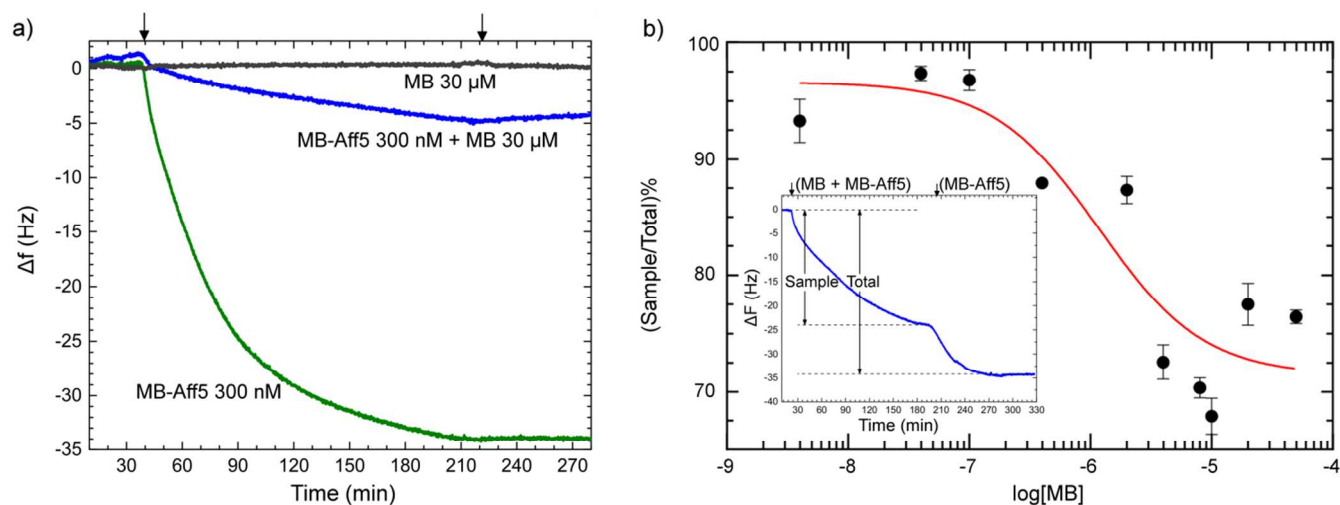
Figure 7. a) Comparison of QCM-D response (F3, third harmonic) between a MB-Aff5 solution and a 1:100 mixture of MB-Aff5 and MB injected over MB:OH SAM-functionalised sensors. As a control, the QCM-D response to a 30 μM MB solution was measured; b) Calibration curve of MB-Aff5 competition assay using QCM-D. Insert shows assay format: QCM-D response (third harmonic) during injection of MB-Aff5+MB mixture, followed by injection of MB-Aff5 until saturation. The first plateau was normalised to the second plateau, (Sample/Total)%.

frequency similar to the blank sample.

MB-Aff5 AFFINITY: A MB:OH SAM-functionalised QCM-D sensor was exposed to increasing concentrations of MB-Aff5 and monitored by QCM-D in order to estimate the Affimer binding affinity. Figure 6a shows the third harmonic of the sensor resonant frequency as a function of time during exposure to MB-Aff5 from 1 μg/mL to 10 μg/mL (PB 7 was injected between samples to remove non-specifically bound material). As the MB-Aff5 concentration increased, the frequency shifts became larger, peaking around 4 μg/mL. The response then saturated at a concentration around 8 μg/mL. The frequency shift was plotted as a function of concentration (insert, Figure 6a) and fitted to a Hill-Langmuir isotherm ($Y = \frac{B_{max} \cdot C^h}{K_D^h + C^h}$), where B_{max} is the maximum response, C is Affimer concentration (nM), h is the hill slope and K_D is the dissociation constant (Supplementary Note 2). K_D was found to be 216.4 nM, comparable to previously reported values for antibodies of small molecules.[22,23]

To study the kinetics of the binding reaction, MB-Aff5 was injected over a MB:OH SAM-functionalised QCM-D sensor at a flow rate of 10 μL/min (Figure 6b and Supplementary Note 3). The rate of association (k_{on}) and dissociation (k_{off}) were found to be 4.1×10⁴ M⁻¹min⁻¹ and 5.6×10⁻⁴ min⁻¹ respectively. Since $K_D = k_{off}/k_{on}$, this yields a dissociation constant of 13.7 nM, which is one order of magnitude lower than that calculated by saturation binding analysis. This discrepancy between kinetic and saturation binding analysis is not uncommon, since, in the latter case, equilibrium is usually not reached within the injection time of reagent at each concentration, which leads to overestimates of the K_D.[23] Thus, the dissociation constant calculated by kinetic analysis is expected to be closer to the true affinity of the binder.

MB-Aff5 COMPETITION ASSAY: Competition assay formats are usually the most appropriate for small-sized targets. The potential of MB-Aff5 binders for analyte de-

tection in competition format was thus assessed using QCM-D. A mixture of 1:100 MB-Aff5:MB in PB 7 was injected over a mixed MB:OH SAM. A second MB:OH SAM-functionalised sensor was treated with a solution containing only MB-Aff5 in order to compare the two signals and investigate the degree of competition between surface-bound MB and free MB for MB-Aff5 binding sites. As seen in Figure 7a, the response from the MB-Aff5:MB mixture was seven times lower than that of the MB-Aff5 baseline, revealing considerable interactions of MB-Aff5 with free MB which competed with that of the surface-bound MB. We note, the injection of a solution of MB at 30 μM in the same buffer yielded no response, thus confirming the absence of non-specific interactions between the monolayer and free MB. Finally, the degree of competition at different MB concentrations was measured through a two-step QCM-D experiment (insert in Figure 7b). First, a mixture of MB and MB-Aff5 was injected over a mixed 1:3 MB:OH SAM-functionalised sensor. The sample was allowed to flow over the surface until the resonant frequency reached a plateau, at which point a solution containing only MB- Aff5 at the same concentration as in the mixture was introduced until a second plateau was reached, corresponding to a surface fully saturated with MB-Aff5.

The first plateau (sample) was then normalised to the second (total/saturated). The process was repeated for a range of different MB concentrations in order to construct a standard curve (Figure 7b). The limit of detection was in the lower μM region. While this is higher than the environmentally relevant concentrations detected by antibody-based ELISAs for small molecules,[24,25] it should be noted that sensitivity in the QCM-D is limited at low concentrations[26], and that the assay has not been optimised. Further study would be required to improve performance, looking for instance, at altering the length of the LCAT-OEG linkers or ratio of the LCAT-OEG-MB and LCAT-OEG-OH dilutant or work out the optimal concentratios of Affimer and surface-immobilised target.

CONCLUSIONS

The challenges of developing bioreceptors for non-immunogenic, small-sized targets were addressed by *in vitro* selection of non-antibody binders using Affimer technology. In this study, Affimers against methylene blue, were developed and fully characterised. Saturation binding and kinetics studies revealed a dissociation constant in the nM region, which is comparable to many small-molecule antibodies. We have also shown that these Affimers exhibit very high selectivity, enabling detection of a specific target molecule from complex aquatic samples. The results presented here clearly demonstrate the potential of *in vitro* selected Affimers for the detection of small-sized, non-immunogenic targets. Based on these promising results, our future work intends to expand the scope of this technology to other pharmaceuticals and emerging environmental contaminants and in the development of simple, inexpensive and high-throughput ELISAs based on Affimer-technology.

ASSOCIATED CONTENT

Supporting information

Biotinylation of MB (NHS/EDC crosslinking reaction and LC-MS spectrum), MB-Affimer protein sequences, Sauerbrey mass estimation, Fitting of Mb-Aff1 and MB-Aff5 saturation binding and kinetics data (QCM-D).

The Supporting Information is available free of charge on the ACS Publications website.

AUTHOR INFORMATION

Corresponding Authors

*Tel: +44(0)1904 32 2693, Fax: +44 (0)1904 32 2335
 E-mail: **steven.johnson@york.ac.uk**   (S.   Johnson),
eleni.koutsoumpeli@york.ac.uk (E. Koutsoumpeli)

Present Addresses

♦J. Murray, Center for Self-assembly and Complexity
Institute for Basic Science, 305-811, Daejeon, South Korea

Notes

The authors declare no competing financial interest.

Author Contributions

E.K. and S.D.J. conceived and designed the QCM-D, PM-IRRAS, CV and EIS experiments and E.K. performed the measurements and calculations. D.C.T, C.T. and A.T. designed and performed the Affimer selection. R.S.B and J.M. elaborated the LCAT-OEG-MB synthesis protocol and contributed to the MB biotinylation protocol. E.K., S.D.J., R.S.B. and D.C.T. contributed to the writing of the manuscript.
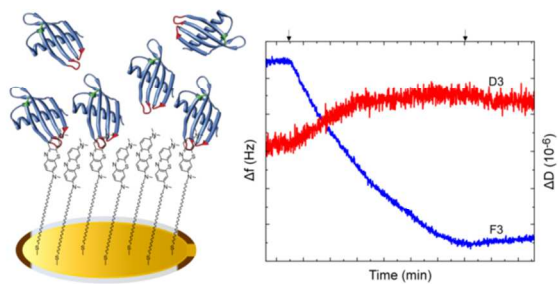
REFERENCES

(1) Bojorge Ramírez, N.; Salgado, A. M.; Valdman, B. *Braz. J. Chem. Eng.* **2009**, *26*, 227-249.

(2) Arugula, M. A.; Simonian, A. *Meas. Sci. Technol.* **2014**, *25*, 032001.

(3) An, Z. *Therapeutic monoclonal antibodies*; John Wiley & Sons: Hoboken, N.J., 2009.

(4) Song, K.; Lee, S.; Ban, C. *Sensors* **2012**, *12*, 612-631.

(5) Tiede, C.; Tang, A. A. S.; Deacon, S. E.; Mandal, U.; Nettleship, J. E.; Owen, R. L.; George, S. E..; Harrison, D. J.; Owens, R. J.; Tomlinson, D. C.; McPherson, M. J. *Protein Eng., Des. Sel.* **2014**, *27*, 145-155.

(6) Rawlings, A.E. ; Bramble, J. P..; Tang, A. A. S..; Somner, L. A.; Monnington, A. E.; Cooke, D. J.; McPherson, M. J.; Tomlinson, D. C.; Staniland, S. S. *Chem. Sci.* **2015**, *6*, 5586-5594.

(7) Sharma, R.; Deacon, S. E.; Nowak, D.; George, S. E.; Szymonik, M. P.; Tang, A. A. S; Tomlinson, D. C.; Davies, A. G.; McPherson, M. J.; Wälti, C. *Biosens. Bioelectron.* **2016**, *80*, 607-613.

(8) Raina, M.; Sharma, R.; Deacon, S. E.; Tiede, C.; Tomlinson, D. C.; Davies, A. G.; McPherson, M. J.; Wälti, C. *The Analyst* **2015**, *140*, 803-810.

(9) Kyle, H. F.; Wickson, K. F.; Stott, J.; Burslem, G. M.; Breeze, A. L.; Tiede, C.; Tomlinson, D. C.; Warriner, S. L., Nelson, A., Wilson, A. J.; Edwards, T.A. *Mol. BioSyst.* **2015**, *11*, 2738-2749.

(10) Coulibaly, B.; Zoungrana, A.; Mockenhaupt, F. P.; Schirmer, R. H.; Klose, C.; Mansmann, U.; Meissner, P. E.; Müller, O., *Plos One* **2009**, *4*, E5318.

(11) Muthuraman, G.; Teng, T. T.; Leh, C. P.; Norli, I. *J. Hazard. Mater.* **2009**, *163*, 363-369.

(12) Murray, J.; Nowak, D.; Pukenas, L.; Azhar, R.; Guillorit, M.; Wälti, C.; Critchley, K.; Johnson, S.; Bon, R. S. J *J. Mater. Chem. B* **2014**, *2*, 3741.

(13) Mrksich, M.Whitesides, G. M. *Poly(ethylene glycol)*; American Chemical Society: Washington DC, 1997; pp. 361-373.

(14) Silin, V.; Weetall, H.; Vanderah, D. J. *J. Colloid Interface Sci.* **1997**, *185*, 94-103.

(15) Koutsoumpeli, E.; Murray, J.; Langford, D.; Bon, R. S. J.; Johnson, S. *Sens. Bio-Sens. Res.* **2015**, *6*, 1-6.

(16) Love, J. C.; Estroff, L. A.; Kriebel, J. K.; Nuzzo, R. G.; Whitesides, G. M. *Chem. Rev.* **2005**, *105*, 1103-1170.

(17) Eckermann, A. L; Feld, D. J.; Shaw, J. A.; Meade, T. J. *Coord. Chem. Rev.* **2010**, *254*, 1769-1802.

(18) Valiokas, R.; Malysheva, L.; Onipko, A.; Lee, H.; Ruželė, Ž.; Svedhem, S.; Svensson, S.; Gelius, U.; Liedberg, B. *J. Electron Spectrosc. Relat. Phenom.* **2009**, *172*, 9-20.

(19) Harder, P.; Grunze, M.; Dahint, R.; Whitesides, G. M.; Laibinis, P. E. *J. Phys. Chem. B* **1998**, *102*, 426-436.

(20) Valiokas, R.; Svedhem, S.; Östblom, M.; Svensson, S. C. T.; Liedberg, B. *J. Phys. Chem. B* **2001**, *105*, 5459-5469.

(21) Dixon, M. *J Biomol Tech.* **2008**, *19*, 151-158.

(22) Kanazawa, K.; Gordon, J. *Anal. Chem.* **1985**, *57*, 1770-1771.

(23) Hulme, E.; Trevethick, M. *Br. J. Pharmacol.* **2010**, *161*, 1219-1237.

(24) Huebner, M.; Weber, E.; Niessner, R.; Boujday, S.; Knopp, D. *Anal. Bioanal. Chem.* **2015**, *407*, 8873-8882.

(25) Marchesini, G. R.; Meulenberg, E.; Haasnoot, W.; Irth, H. *Anal. Chim. Acta* **2005**, *528*, 37-45.

(26) Q-Sense Services - Biolin Scientific http://www.biolinscientific.com/q-sense/services/ (accessed Oct 22, 2016).

For Table of Contents only